

Optofluidics and Optoelectronic Tweezers

Arash Jamshidi, Aaron T. Ohta, Justin K. Valley, Hsan-Yin Hsu, Steven L. Neale, and Ming C. Wu

Department of Electrical Engineering, University of California, Berkeley, CA 94720

ABSTRACT

Optofluidics¹ is the process of integrating the capabilities of optical and fluidic systems to achieve novel functionalities that can benefit from both. Among the novel capabilities that an optical system can bring to the table is the ability to manipulate objects of interest in a liquid media. In the case of biological samples, the objects of interest consist mainly of cells and viruses, whereas in applications such as nanoelectronics, manipulation of nanoparticles is of interest. In recent years, optoelectronic tweezers² (OET) has emerged as a powerful technique for manipulation of microscopic particles such as polystyrene beads, cells, and other biological samples and nanoscopic objects such as nanowires.

In this paper, we will focus mostly on recent advances in the optoelectronic tweezers technology, including characterization of optoelectronic tweezers operational regimes, manipulation of biological samples such as cells in high-conductivity physiological solutions with translation speeds higher than $30 \mu\text{m/s}$ ³, manipulation of air bubbles in silicone oil media with speeds up to 1.5 mm/s ⁴, and exploring the limits on the smallest particle that OET is capable of trapping⁵. These advances all contribute immensely to the functionalities of OET as an optofluidic system.

Keywords: Optoelectronic tweezers, Optofluidics, Optical manipulation, Dielectrophoresis, Droplet manipulation.

1. INTRODUCTION

1.1 Optoelectronic tweezers principles of operation

There has been much progress in last few decades to create novel techniques for manipulation of microscopic and nanoscopic objects. However, in the field of *optical* manipulation, only two technologies have emerged as most influential. The first technique, called optical tweezers, invented by Ashkin et al.^{6, 7}, takes advantage of the optical gradient force of a highly focused laser source to interact with particles in the solution. Optical tweezers have proved to be a very effective tool for study of and interaction with different biological and nanoscale objects. However, to create a stable trap, optical tweezers require very high optical power intensities which limit their effectiveness in performing high-throughput and large-scale optical manipulation functions. The second technique, called optoelectronic tweezers² (OET), is an optically-controlled manipulation technique that works based on the principle of light-induced dielectrophoresis force, which is an electrical gradient force. In this technique, it is not the optical field that is performing the manipulation directly; it is the electric field gradient created by the interaction of the optical field with a photoconductive material that is trapping the objects. Therefore, OET is capable of manipulating objects with optical power intensities that are approximately 5 orders of magnitude smaller than optical tweezers, and as a result, OET is more easily implemented for large-scale, high-throughput optical manipulation functions.

Fig. 1 shows the structure of the optoelectronic tweezers (OET) device. The OET device consists of a top transparent indium-tin-oxide (ITO) electrode and a bottom ITO-coated glass substrate on top of which there is a 1- μm -thick layer of photoconductive material (hydrogenated amorphous silicon, a-Si:H). The liquid solution containing the particles of interest is sandwiched between the top and bottom surfaces and an AC voltage is applied between the top and bottom ITO electrodes. A light source is used to interact with the photoconductive surface and manipulate the objects. The manipulation principle is as follows: when there is no light source present, the impedance of the photoconductive layer is higher than the impedance of the liquid layer, therefore, the majority of the applied AC voltage is dropped across the photoconductive layer. However, in the presence of a light source, electron-hole pair carriers are generated in the photoconductive material and the impedance of the photoconductive layer is reduced, causing the majority of the AC voltage to drop across the liquid layer. It is important to note that the impedance of the photoconductive layer is only

reduced in the area that the light source is present. Therefore, the electric field created in the liquid layer has a non-uniform profile.

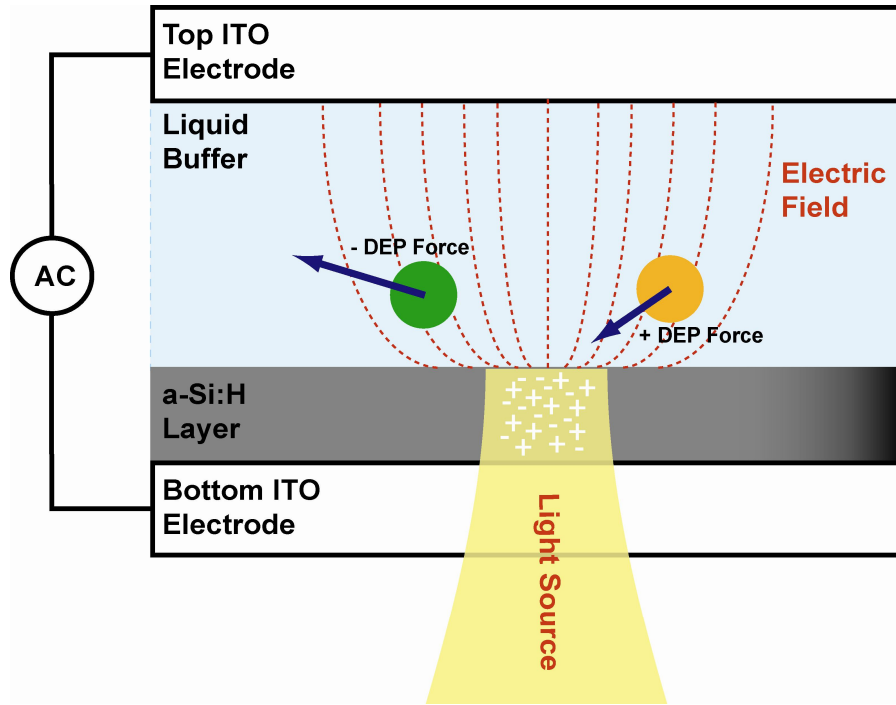


Fig. 1: Optoelectronic tweezers (OET) device structure. The OET device consists of a top transparent ITO electrode and a bottom ITO electrode. There is a layer of photoconductive material (hydrogenated amorphous silicon) on top of the bottom electrode. An AC voltage is applied between the two electrodes. The interaction of the light source with the photoconductive layer reduces the impedance locally, transferring the voltage to the liquid layer in the area that the light is present. This non-uniform electric field traps the particles by light-induced dielectrophoresis. The particles are either attracted (+ DEP force) or repelled (- DEP force) to areas of highest electric field gradient based on their relative properties to the liquid medium.

Once the non-uniform electric field is created in the liquid layer, this field interacts with the dispersed particles and polarizes them; however, since the field is non-uniform, the amount of polarization on two ends of the particle is unequal. Thus, there will be a net force on the particles that will move them towards or away from areas of highest electric field gradient, depending on their relative material properties to the liquid medium. The force on the particles is called dielectrophoresis (DEP) and can be summarized in the following formulation⁸:

$$F_{DEP} = 2\pi r^3 \epsilon_m \operatorname{Re}\{K^*(\omega)\} \nabla E_{rms}^2$$

$$K^*(\omega) = \frac{\epsilon_p^* - \epsilon_m^*}{\epsilon_p^* + 2\epsilon_m^*}, \epsilon_m^* = \epsilon_m - j \frac{\sigma_m}{\omega}, \epsilon_p^* = \epsilon_p - j \frac{\sigma_p}{\omega}$$

where r is the radius of the particle, ϵ_m and ϵ_p are the permittivities of the media and the particle respectively, σ_m and σ_p are the conductivities of the media and the particle respectively, ω is the frequency of the AC potential, $\operatorname{Re}\{K^*(\omega)\}$ is the real part of the Clausius-Mossotti (C.M.) factor $K^*(\omega)$, and ∇E^2 is the gradient of the squared electric field. The C.M. factor is a function of the permittivity and conductivity of the particle and the media, and in the case of spherical particles, has a value between -0.5 and 1. For a positive C.M. factor, the particles are more polarizable than the media and experience a positive DEP force towards areas of highest electric field gradient; for a negative C.M., the particle experience a negative DEP force away from areas of highest electric field gradient.

Optoelectronic tweezers has already proven to be a strong manipulation tool for micro-scale particles such as cells and polystyrene beads. For example, it has been shown² that OET is capable of massively parallel manipulation of 15,000 particles over a large area, 1.3 mm by 1.0 mm. In addition, OET is capable of manipulation of various types of cells and separation of dead and live cells. Moreover, the low optical power density required for trapping particles makes OET well suited for the manipulation of biomolecules. In addition, the ability to create real-time dynamic OET virtual electrodes makes it an extremely flexible tool capable of addressing individual particles over a large manipulation area. These capabilities are essential in making OET a versatile optofluidic system. In the next section, we are going to explore some of the new advances of OET in recent years that expand the capabilities of OET as an optofluidic system even further.

2. RECENT ADVANCES IN OPTOELECTRONIC TWEEZERS

2.1 Characterization of OET operational regimes

Even though the main operational principle of OET has been the light-induced dielectrophoresis (DEP) principle, there are other operational regimes in the OET device that can be used⁹. A comprehensive understanding of these operational regimes is essential in using OET as an integral part of an optofluidic system. Three main operational regimes of OET include: dielectrophoresis (DEP), electro-thermal flow, and light-actuated AC electro-osmosis¹⁰ (LACE). The different operational regimes can be achieved in OET by tuning the parameters such as optical power and frequency. Fig. 2 shows the dominant effect in OET as a function of optical power and frequency.

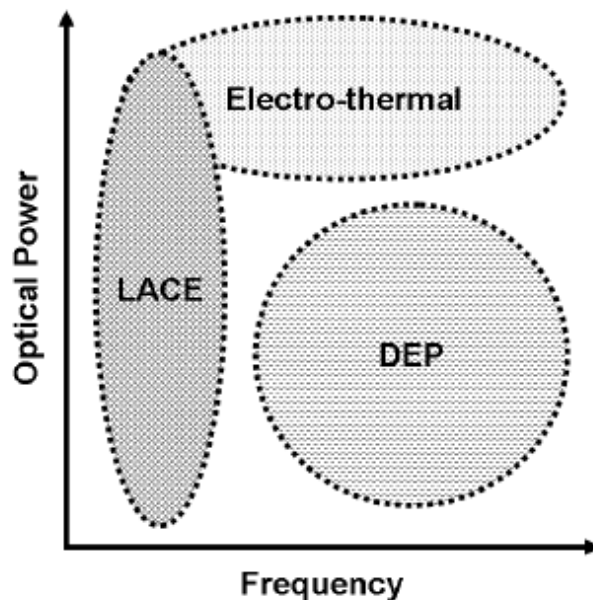


Fig. 2: OET operational regimes as a function of optical power and frequency.

The DEP operational regime is as discussed in the previous section. In this section, we will focus on the electro-thermal and LACE effects. The electro-thermal flow is an effect due to a temperature gradient present in the liquid layer created by the absorption of the light source in the photoconductive material. This effect is only observed at very high optical power intensities of more than 100 W/cm^2 , which is much larger than typical optical power intensities used for trapping. The electro-thermal flow is mostly a parasitic effect and is not capable of trapping any objects; however, due to the very high optical powers necessary to achieve this operational regime, it does not interfere with typical OET operation.

The other effect that has been observed in OET is called light-actuated AC electro-osmosis or LACE. At lower frequencies, the lateral component of the electric field created in the liquid layer interacts with the double-layer charges on the surface of the OET device virtual electrodes and can accelerate them laterally, creating a flow vortex around the light source (Fig. 3a). This effect is typically observed at frequencies smaller than 10 kHz and can be used for trapping

nano-scale objects such as polystyrene beads as small as 200 nm (Fig. 3b,c). Using this method, it has been demonstrated that 31,000 individually addressable traps can be created for particle larger than 1 μm in diameter¹⁰. This trapping mechanism is essentially independent of particle properties which makes it an attractive choice for manipulation and trapping of nanoparticles.

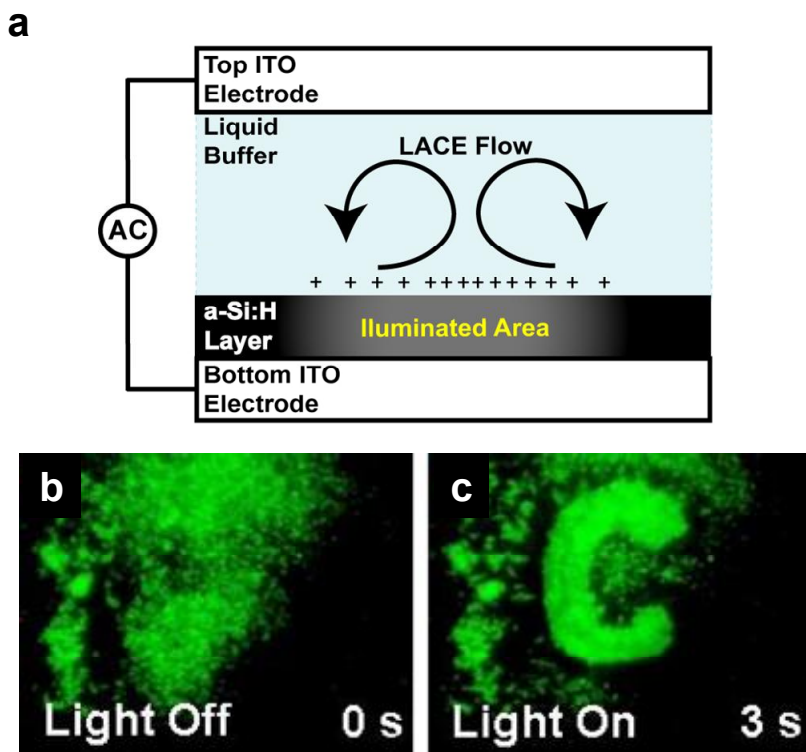


Fig. 3: (a) Light-actuated AC electro-osmosis (LACE) flow pattern created in the vicinity of a light pattern virtual electrode. The lateral component of the electric field interacts with the double layer charges on the illuminated area, therefore, driving the liquid in a vortex pattern around the light source. (b,c) LACE trapping of 200 nm polystyrene beads over a period of 3 seconds. A light pattern in the form of a C character is projected on the OET substrate using a spatial light modulator, forming a virtual electrode for LACE trapping of the particles.

2.2 Optical manipulation of biological objects

One of the most important applications of OET is its ability to manipulate cells and other biological samples in the liquid media with optical intensities orders of magnitude smaller than optical tweezers, minimizing harmful effects on the cells. Previously, OET has been used for manipulation of red and white blood cells^{11, 12} and separation of live and dead human B cells². However, conventional OET devices with hydrogenated amorphous silicon as the photoconductive layer have been limited to manipulation of particles in liquid conductivities smaller than 100 mS/m. This limitation arises from the fact that conventional OET is incapable of effectively switching the AC voltage from the photoconductive layer to the liquid layer due to relatively small photoconductivity of the amorphous silicon layer.

The ability to perform cell manipulation in a high conductivity physiological solution is essential for maintaining cell viability¹³ and performing other applications such as cell electroporation. To overcome this limitation of the conventional OET device, it is possible to replace amorphous silicon as the photoconductive layer with an N⁺PN phototransistor structure which has more than 2 orders of magnitude larger photoconductivity due to the higher carrier mobility in single crystalline silicon and the phototransistor current gain. This novel OET device is called phototransistor OET (phOET). Fig. 4a shows the phOET device structure consisting of a top transparent ITO electrode and a bottom N⁺PN phototransistor structure with an AC bias applied between the top and bottom surfaces. The liquid layer containing the particles of interest is sandwiched between the two surfaces.

It has been demonstrated³ that phOET is capable of transporting HeLa and Jurkat cells with speeds higher than 30 $\mu\text{m}/\text{s}$ in phosphate-buffered saline solution (PBS) and Dulbecco's Modified Eagle Medium (DMEM) solutions, with conductivities of 1.5 S/m. PhOET is typically operated at frequencies in MHz regime which translates to a negative

dielectrophoresis force for the trapped cells, moving them away from areas of highest electric field gradient. Fig. 4b shows the transport of two HeLa cells in a PBS solution using a phOET device.

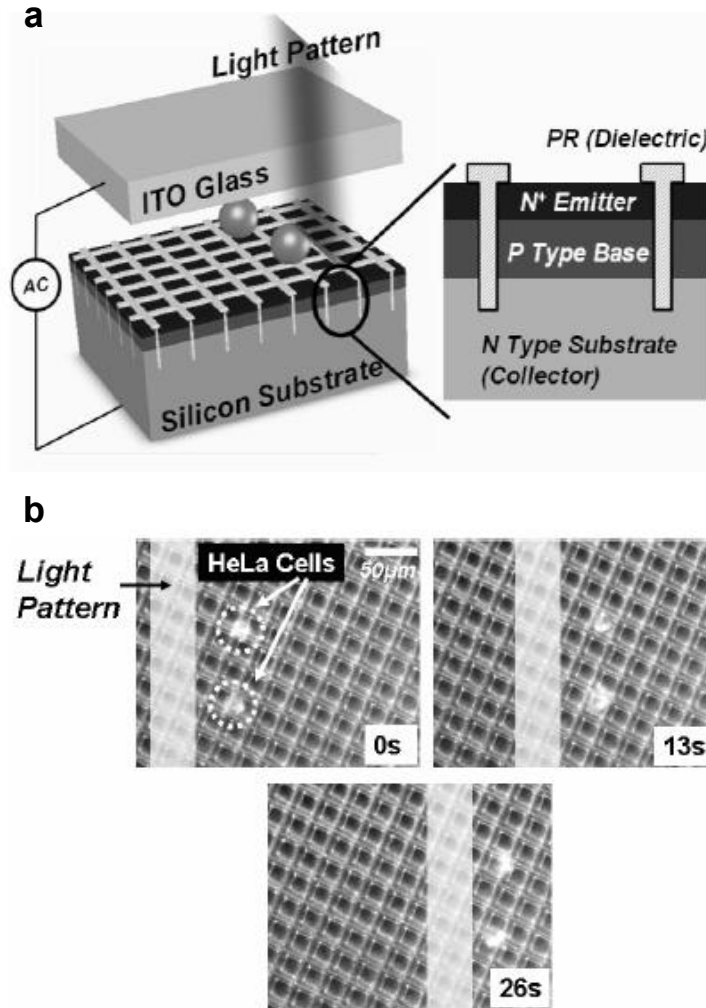


Fig. 4: (a) Phototransistor OET (phOET) device structure. The phOET device structure resembles the conventional OET structure (Fig. 1) with the exception that the photoconductive layer is replaced by an N^+PN phototransistor structure. The larger carrier mobility and higher transistor gain of this layer enables phOET to trap cells in their high-conductivity physiological solutions. (b) Transport of two HeLa cells in a PBS solution using the phOET.³ (This figure is a reproduction from reference 3 with permission © IEEE).

2.3 Thermocapillary movement of air bubbles

The ability to move air bubbles is another important functionality required in a versatile optofluidic system. Air bubbles have been used for a variety of applications such as mixers¹⁴, valves¹⁵, pumps¹⁶, and performing Boolean logic¹⁷. The bubbles can be either passively positioned using fluidics or actively positioned using various methods such as dielectrophoresis¹⁸, electrowetting¹⁹, optoelectrowetting²⁰, evaporation²¹, and thermal gradient²². Conventionally, thermal gradients have been created using resistive heating elements. However, it has been demonstrated²³ that it is possible to create the necessary temperature gradients for thermocapillary manipulation of bubble using a light source.

Optically controlled actuation of the thermocapillary force has several advantages over other conventional methods including: flexible and reconfigurable manipulation capability and convenient control of a large number of bubbles. This optically-controlled thermocapillary force can be created in a conventional OET device by using the photoconductive substrate as an absorber of the light energy which results in the formation of a temperature gradient in the liquid layer. This temperature gradient in turn creates a surface tension gradient in the liquid, leading to a flow pattern from warmer areas towards the colder areas to minimize the energy. Therefore, the bubbles move to high

temperature gradient areas and are stably trapped in the illuminated area. Fig. 5 shows the optically-induced thermocapillary trapping of a 109- μm -diameter air bubble in a silicone oil media. The air bubble follows the position of the laser trap as it is scanned across the stage over a period of 12 s.

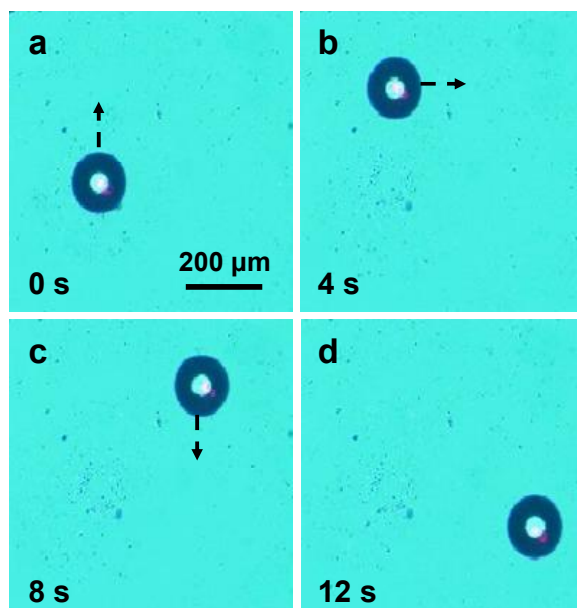


Fig. 5: (a-d) Optically actuated thermocapillary transport of an air bubble in silicone oil. A 109 μm -diameter bubble is trapped in the thermal trap created by a laser. The bubble follows the position of the laser spot as it is scanned across the stage⁴.

This method has been used to transport bubbles with diameters ranging from 33 to 329 μm (corresponding to 19 pl – 23 nl). The translation speed of the bubbles is a linear function of optical power intensity used, since the laser intensities are directly proportional to temperature gradients. The translation speed for bubbles less than 0.5 nl can reach 1.5 mm/s with 2 kW/cm^2 optical intensity.

2.4 OET for nanoparticle manipulation

The bottom-up approach is one of the main methods of organizing nano-scale objects. In this method, nano-scale building blocks such as nanowires, gold nanoparticles, and carbon nanotubes are put together to form structures with more complex functionalities. Current advances in the synthesis²⁴ of nanoscopic materials have created an array of objects with interesting compositions and properties. Several methods including fixed electrode dielectrophoresis^{25,26} (DEP) and optical tweezers^{27,28} have already been used for manipulation of nanowires and carbon nanotube. However, in the case of fixed-electrode DEP, the trapping patterns are fixed which prevent dynamic and flexible manipulation of trapped nanowires, and in the case of optical tweezers, the high optical power intensities required for stable trapping limit the working area. Optoelectronic tweezers can overcome both these challenges by trapping and manipulation of nanostructures using virtual electrode patterns created at low optical power intensities⁵.

As mentioned before, the magnitude of the dielectrophoresis force scales with the volume of the particle. Therefore, trapping of objects using the dielectrophoresis gets more and more challenging as the size of the particle becomes smaller. Previously, the smallest particles that OET was capable of trapping was 1- μm -diameter polystyrene beads. However, in the case of cylindrical nanostructures such as nanowires, the magnitude of the DEP force is enhanced due to one dimension of the wires (length) being in micrometer scale and higher polarizability of the particles which leads to a larger C.M. factor. The combination of these two factors cause the magnitude of the DEP force experienced by a nanowire to be more than 2 orders of magnitude larger than a spherical particle with comparable diameter. It has been demonstrated⁵ that OET is capable of trapping and transport of nanowires with diameters below 20 nm and approximately 5 μm in length. The trapped nanowires can be of a variety of compositions including silicon, gallium nitride, and silver.

Fig. 6a shows the experimental setup for trapping an individual silicon nanowire. A 10 mW, 633 nm diode laser source is attenuated to 100 μW and focused onto the OET chip using a 40X objective lens. A dark-field condenser is used for observation of the scattered light from the nanowires. Figs. 6b-d show the process of trapping an individual

silicon nanowire using a laser source. In the beginning, there is no voltage applied to the device and the nanowire is undergoing Brownian motion, however, once the voltage is applied (Fig. 6c) the long axis of the nanowire aligns with the electric field, the nanowire experiences a positive DEP force and is attracted to the trapping source, transported by manually adjusting the position of the trapping source.

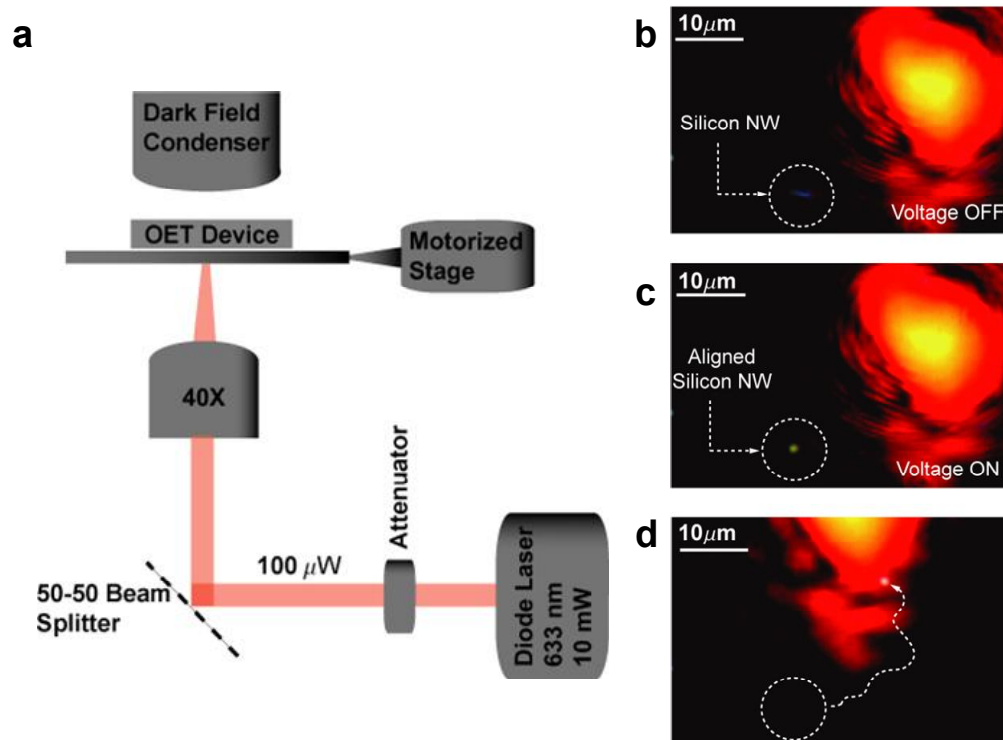


Fig. 6: (a) Experimental setup for manipulation of silicon nanowires. A 10-mW HeNe laser was attenuated to 100 μ W and focused onto the OET chip for manipulation of nanowires using a 40X objective lens. (b-d) Trapping of an individual silicon nanowire using a laser spot; (b) No voltage is applied across the device, and the nanowire undergoes Brownian motion; (c) The voltage is applied, and the long-axis of the nanowire aligns with the electric field; (d) The nanowire experiences a positive DEP force and follows the trap.

In addition to using a single source laser trap, it is possible to use a digital micromirror display (DMD) to create multiple traps in real-time that can be controlled using a computer interface. Fig. 7 shows the process of creating 2 \times 3 array of individual silicon nanowires using a DMD. Each trapped nanowire is individually addressable and can be dynamically positioned in real-time.

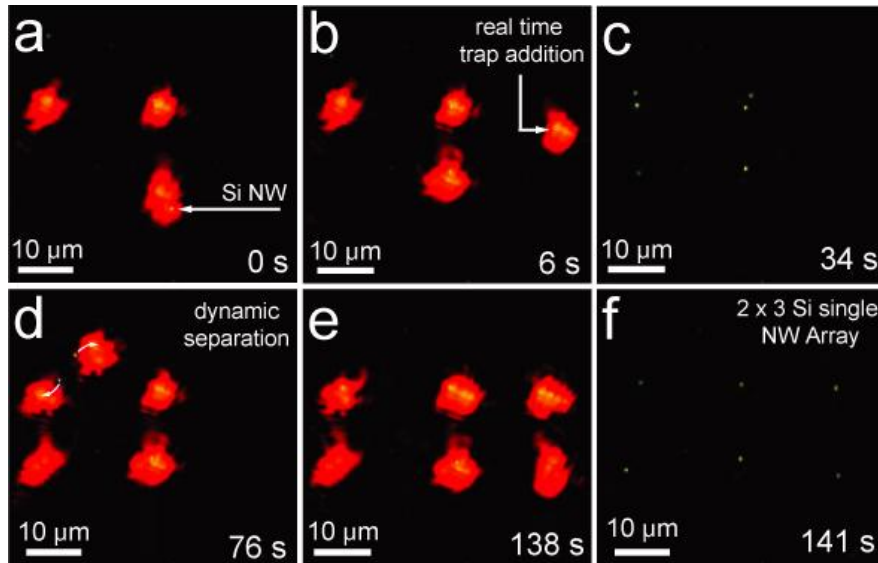


Fig. 7: Arrangement of six individual silicon nanowires into a 2×3 array using traps created with a digital micromirror device (DMD) and positioned using a computer interface. (a) An individual silicon nanowire moving into the lower laser trap. (b) Real-time trap addition. (c) The trapping laser is filtered to show the top traps that each contain two silicon nanowires. (d) To create a single nanowire array, a new trap is added to separate the nanowires in top left corner. (e) The 2×3 single nanowire array, (f) with filtered laser pattern. (This figure is a reproduction from reference 5 (supporting information) with permission © Nature Publishing Group).

In addition to trapping individual nanowires, OET is capable of separating nanowires based on their material properties⁵. As mentioned before, OET works based on the dielectrophoresis principle which depends on the polarizability of the particles. Due to their higher conductivities, silver nanowires are more polarizable than silicon nanowires and they experience a larger DEP force than silicon nanowires. Therefore, by adjusting the trapping AC voltage, it is possible to tune the translation speed of a trapping source so that the silver nanowires stay trapped while silicon nanowires fall as the laser source is scanned over the surface and therefore effectively separate silicon and silver nanowires. This separation capability can be important in many areas including the separation of metallic and semiconducting carbon nanotubes which is one of the main challenges in the area of nanoelectronics²⁵.

3. CONCLUSION

In conclusion, OET is an optically controlled manipulation technique for large-scale and flexible manipulation of microscopic (such as cells and polystyrene beads) and nanoscopic (such as nanowires) objects. Due to its trapping flexibility, low required optical power intensity, and large working area, OET has already proven to be a very attractive tool for the manipulation of various objects. In this review paper, we discussed some of the recent advances in the optoelectronic tweezers technology including: complete characterization of OET operational regimes including light-actuated AC electro-osmosis (LACE), dielectrophoresis (DEP), and electro-thermal flow effects, manipulation and trapping of cells in high conductivity physiological solutions with translation speeds higher than $30 \mu\text{m/s}$ using a novel phototransistor OET (phOET) device, trapping and transport of air bubbles in a silicone oil media with speeds as high as 1.5 mm/s , and manipulation, separation, and organization of semiconducting and metallic nanowires with diameters below 20 nm . These advances further enhance OET's capability as a versatile optofluidic system for manipulation and study of cells and other biological samples, trapping and manipulation of air bubbles for a variety of applications in optofluidics including Boolean logic, and organization, separation, and trapping of nanostructures for applications in nanoelectronics and nano-optics.

4. ACKNOWLEDGEMENT

This work was supported in part by the National Institutes of Health through the NIH Roadmap for Medical Research (Grant #PN2 EY018228), DARPA UPR-CONSRT, DARPA (HR 0011-07-1-0037), and the Institute for Cell Mimetic Space Exploration (CMISE). A.T.O. thanks the NSF for a graduate research fellowship.

5. REFERENCES

- [1] Psaltis, D., Quake, S. R. & Yang, C., "Developing optofluidic technology through the fusion of microfluidics and optics," *Nature* 442, (2006).
- [2] Chiou, P. Y., Ohta, A. T. & Wu, M. C., "Massively parallel manipulation of single cells and microparticles using optical images," *Nature* 436, 370-372 (2005).
- [3] Hsu, H.-Y., Ohat, A. T., Chiou, P. Y., Jamshidi, A. & Wu, M. C., "Phototransistor-Based Optoelectronic Tweezers for Cell Manipulation in Highly Conductive Solution," in the 14th International Conference on Solid-State Sensors, (2007).
- [4] Ohta, A. T., Jamshidi, A., Valley, J. K., Hsu, H.-Y. & Wu, M. C., "Optically actuated thermocapillary movement of gas bubbles on an absorbing substrate," *Applied Physics Letters* 91, (2007).
- [5] Jamshidi, A. et al., "Dynamic manipulation and separation of individual semiconducting and metallic nanowires," *Nature Photonics* 2, (2008).
- [6] Ashkin, A., "Acceleration and Trapping of Particles by Radiation Pressure," *Physical Review Letters* 24, 156 (1970).
- [7] Ashkin, A., Dziedzic, M. & Yamane, T., "Optical trapping and manipulation of single cells using infrared-laser beams," *Nature* 330, 769-771 (1987).
- [8] Jones, T. B., [Electromechanics of Particles], Cambridge University Press, (1995).
- [9] Valley, J. K., Jamshidi, A., Ohat, A. T., Hsu, H.-Y. & Wu, M. C., "Operational Regimens and Physics Present in Optoelectronic Tweezers," *Journal of Microelectromechanical Systems* DOI 10.1109, (2008).
- [10] Chiou, P. Y., Ohta, A. T., Jamshidi, A., Hsu, H.-Y. & Chou, J. W., M. C., "Light-actuated AC electroosmosis for optical manipulation of nanoscale particles," in Proceedings of Solid-State Sensor, Actuator, and Microsystems Workshop, 56-59 (2006).
- [11] A. T. Ohta, P. Y. Chiou, H. L. Phan, S. W. Sherwood, J. M. Yang, A. N. K. Lau, H.-Y. Hsu, A. Jamshidi, and M. C. Wu, "Optically-controlled cell discrimination and trapping using optoelectronic tweezers," *IEEE Journal of Selected Topics in Quantum Electronics* 13(2), 235-243 (2007).
- [12] A. T. Ohta, P. Y. Chiou, T. H. Han, J. C. Liao, U. Bhardwaj, E. R. B. McCabe, F. Yu, R. Sun, and M. C. Wu, "Dynamic cell and microparticle control via optoelectronic tweezers," *IEEE Journal of Microelectromechanical Systems* 16(3), 491-499 (2007).
- [13] Voldman, J., "Electrical forces for microscale cell manipulation," *Annual Review Of Biomedical Engineering* 8, 425-454 (2006).
- [14] Garstecki, P., Fuerstman, M. J., Fischbach, M. A., Sia, S. K. & Whitesides, G. M., "Mixing with bubbles: a practical technology for use with portable microfluidic devices," *Lab Chip* 6, (2006).
- [15] Hua, S. Z., Sachs, F., Yang, D. X. & Chopra, H. D., "Microfluidic actuation using electrochemically generated bubbles," *Anal. Chem.* 74, (2002).
- [16] Jun, T. K. & Kim, C. J., "Microscale Pumping with Traversing Bubbles in Microchannels," *J. Appl. Phys.* 83 (1998).
- [17] Prakash, M. & Gershenfeld, N., "Microfluidic Bubble Logic," *Science* 315, (2007).
- [18] Schwartz, J. A., Vykoukal, J. V. & Gascoyne, P. R. C., "Droplet-based chemistry on a programmable micro-chip," *Lab Chip* 4, (2004).
- [19] Pollack, M. G., Shenderov, A. D. & Fair, R. B., "Electrowetting-based actuation of droplets for integrated microfluidics," *Lab Chip* 2, (2002).
- [20] Chiou, P. Y., Moon, H., Toshiyoshi, H., Kim, C. J. & Wu, M. C., "Light actuation of liquid by optoelectrowetting," *Sens. Actuators* 104, (2003).
- [21] Liu, G. L., Kim, J., Lu, Y. & Lee, L. P., "Optofluidic control using photothermal nanoparticles," *Nat. Mater.* 5, (2006).
- [22] Kataoka, D. E., "Patterning liquid flow on the microscopic scale," *Nature* 402, (1999).
- [23] Kotz, K. T., Noble, K. A. & Faris, G. W., "Optical microfluidics," *Applied Physics Letters* 85, (2004).
- [24] Yang, P. D., "The Chemistry and Physics of Semiconductor Nanowires," *MRS Bulletin* 30, 85-91 (2005).
- [25] Krupke, R., Hennrich, F., von Lohneysen, H. & Kappes, M. M., "Separation of metallic from semiconducting single-walled carbon nanotubes," *Science* 301, 344-347 (2003).
- [26] Smith, P. A. et al., "Electric-field assisted assembly and alignment of metallic nanowires," *Applied Physics Letters* 77, 1399-1401 (2000).
- [27] Agarwal, R. et al., "Manipulation and assembly of nanowires with holographic optical traps," *Optics Express* 13, 8906-8912 (2005).

[28] Pauzauskis, P. J. et al., "Optical trapping and integration of semiconductor nanowire assemblies in water," *Nature Materials* 5, 97-101 (2006).